Macromolecules

Article

Cite This: *Macromolecules* XXXX, XXX, XXX−XXX

pubs.acs.org/Macromolecules

Double Reversible Networks: Improvement of Self-Healing in Hybrid Materials via Combination of Diels−Alder Cross-Linking and Hydrogen Bonds

Sandra Schäfer and Guido Kickelbick*

Inorganic Solid State Chemistry, Saarland University, Campus C4$_1$, 66123 Saarbrücken, Germany

Supporting Information

ABSTRACT: Intrinsic self-healing materials rely on a reversible bond formation after failure. In this study we report hybrid materials that contain two intrinsic self-healing forces: The reversible covalent bond formation of Diels−Alder groups is supported by intrinsic hydrogen bonds, which form supramolecular interactions and contribute to the mobility and proximity of the DA groups. This concept was realized by a combination of urea group containing spherosilicates with butyl methacrylate based polymers bearing both DA moieties and self-assembling hydrogen bonds. Multifunctional one-component polymers were synthesized and studied regarding their application in self-healing hybrid materials. The self-healing behavior was investigated following the signals for bond release and formation of DA groups in the material using IR, UV-vis, and CP-MAS NMR spectroscopy. Furthermore, DSC and rheological measurements were performed and revealed that the materials are superior compared to previously studied systems concerning their healing capacity. The self-healing behavior of the formed hybrid materials was proven by a cut healing test of several millimeters using microscope images. We can conclude that it is advantageous to combine several reversible functions in one material to promote the self-healing capacity particularly in nanocomposites where the flexibility of the network is restricted.

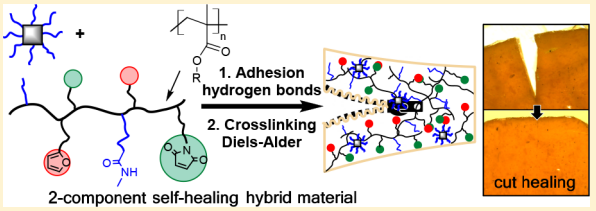

1. INTRODUCTION

Intrinsic self-healing materials are based on reversible bond formation on the molecular scale, which requires quite flexible polymer structures to foster the connectivity of damaged surfaces. This is necessary for the re-formation of the bonds, which only takes place at the nanometer scale or below, when the proximity of reactants is reached.[1] During the past two decades the Diels−Alder (DA) reaction was identified as one of the most promising reaction types in polymer self-healing materials.[2] The thermoreversible [4 + 2] cycloaddition between electron-rich dienes and electron-deficient dienophiles, like furan and maleimide, works at temperatures between 100 and 150 °C and thus in a region that allows its use in daily applications.

Generally chain diffusion, in particular the mobility of functional groups, is one of the most important parameters with respect to the ability to heal intrinsic systems. Regarding self-healing nanocomposites compared to polymers, additional challenges have to be considered. Inorganic fillers increase, for example, hardness and T_g, but both are disadvantageous for the previously described requirements concerning healing mechanisms. Furthermore, there is a huge difference between the usage of fibers or particles as the inorganic moiety in such composites. While fibers can break or change their alignment,[3] which cannot be reorganized applying polymer healing mechanisms, spherical particles or large isotropic molecules have no translational preferred direction, are not aligned, and do not tend to break because of brittleness within the softer matrix. Because of these multiple challenges only a few studies have been conducted in self-healing nanocomposites based on DA cross-linking. Generally the organic polymers and the inorganic moieties have to be optimized for the best performing nanocomposites or hybrid materials. Several research groups already studied polymer nanocomposites based on click chemistry reactions[4−6] and revealed that MWCNT's (multiwalled carbon nanotubes), GO (graphene oxide), or inorganic NPs (SiO_2) have a potential in self-healing nanocomposites. Careful control of the chemical surface modification is necessary for a homogeneous distribution of inorganic nanoparticles in organic polymers.

A few studies have been conducted using SiO_2 nanoparticles in DA based healing composites. Chujo et al. synthesized a 20% furan modified polystyrol, which was reacted *in situ* with tetraethyl orthosilicate and a maleimido alkoxysilanes.[7] This procedure resulted under appropriate conditions a colorless, transparent hybrid material that revealed retro-Diels−Alder (rDA) reactions in DSC. In our group a system was developed in which a grafting-from polymerization applying SI-ATRP was used to modify 40 nm SiO_2 with a copolymer of butyl methacrylate and 10 mol % protected maleimidoethyl methacrylate. These particles were incorporated in the corresponding furan and butyl methacrylate group containing

Received: March 20, 2018
Revised: June 25, 2018

DOI: 10.1021/acs.macromol.8b00601
Macromolecules XXXX, XXX, XXX−XXX

polymers to form a self-healing composite, which is able to heal scratches on a micrometer scale.[8] For a deeper understanding of the limiting parameters when reacting molecular surface functionalized particles with the corresponding molecules[9] or different matrices,[10] in particular siloxanes and poly(butyl methacrylate)s (pBMA), a study using different spacer lengths was conducted. While the pBMA samples showed no conversion in DSC, the elastomers indicated a conversion. This leads to the assumption that again the mobility of functional groups and also the flexibility of the matrix are the key for effective healing. In a recent study we developed a system based on spherical magnetite/maghemite nanoparticles, which was modified using a monolayer of phosphonic acids on the surface.[11] Reacting these particles with different types of molecules, we found that the sterical demand of the attacking reagent is the limiting factor in this type of materials rather than the crowdedness of the surface. This result is further supported by the observation that smaller molecular inorganic building blocks lead to a faster healing in the nanocomposites. Thus, spherosilicate or silsesquioxane based DA systems heal more efficiently than the ones with SiO_2 nanoparticles. Liu et al. described an octamethyl methacrylate modified POSS (polymeric octahedral silsesquioxane) which was reacted with furfurylamine.[12] A partially thermoreversible network was formed via the reaction of the methacrylate double bond with either the amine in a Michael addition or the furan in a DA reaction. Lin et al. described an octafurfurylamine POSS, which was cross-linked using the commercial 1,1′-(methylenedi-4,1-phenylene)bismaleimide (BMI) and formed a curable solid.[13] We described furan modified spherosilicates prepared via hydrosilylation, which were incorporated in BMI or linear maleimide siloxanes and resulted in hybrid materials that showed a high conversion in DA reactions.[14] Zelisko et al. also synthesized furan modified spherosilicates cross-linked with maleimide siloxanes starting from different precursors and found an intrinsically healing system.[15]

Besides DA cross-linking reactions also other interaction types were used for intrinsic healing systems. For example, spontaneous supramolecular assembly by a hydrogen bond donor−acceptor interaction results in a fast reconnection of surfaces. Although individual hydrogen bonds are weak, collectively they form a strong network that is dynamic at room temperature[16] and allow autonomic healing. Liu et al. studied solvent induced healing of PMMA at 40−60 °C and found that, in addition to mechanical lock of the broken chains, hydrogen bonds promoted the mechanical strength of the healed sample because of the interaction between methanol and broken polymeric chains.[17]

According to the literature, chemical networks show a kind of molecular memory when covalent and supramolecular groups are combined.[18] Weaker hydrogen bonds can break and build again spontaneously, while covalent bonds provide the basic stability and robustness.

Probably the first who studied the combination of DA and hydrogen bonds was the group of Picchioni.[19,20] The first attempt was the chemical modification of aliphatic polyketones with furan and primary amines. The polymers were cross-linked with commercial bismaleimides. The incorporation of hydrogen bonds between amine and carbonyl groups leads to a significant increase in T_g and thus extends the possible application of the material. One drawback in this polymeric material is the side reaction between amine and carbonyl groups, which leads to irreversible links.[19] In a subsequent study, this drawback was overcome by OH-group containing derivatives instead of amines.[20] In 2017, Raquez et al. reported one-component DA based polyurethanes and achieved a free-standing healable film, when an appropriate ratio of hydrogen bonds to DA functions was adjusted.[21]

In this work, intrinsic healing hybrid materials that contain two types of independent reversible interactions are investigated. Physical hydrogen bonds, which can form spontaneously and are located in the matrix and on the surface of the inorganic moiety, provide the ideal miscibility and homogeneous distribution of the filler. Covalent bonds, which can be thermally triggered by the DA reaction, are located only in the polymer chains to ensure good mobility and accessibility of these groups. One-component polymers, bearing diene, dienophile, and amide or urea groups, were synthesized using controlled radical polymerizations (CRPs). ATRP (atom transfer radical polymerization), ARGET ATRP (activator regenerated by electron transfer), and RAFT (reversible addition−fragmentation chain transfer) were performed with a mixture of previously synthesized monomers. The resulting linear poly(butyl methacrylates) contain maleimide, furan, and hydrogen bond moieties at the same backbone. Octaurea-functional spherosilicates[22] were chosen as inorganic moiety, as they are molecular, soluble, three-dimensional nanobuilding blocks. The received materials showed a superior self-healing potential according to DSC measurements and microscope images.

2. EXPERIMENTAL SECTION

Materials. $CuBr_2$ (99%), hydrazine hydrate solution in H_2O (78−82%), 2-cyano-2-propyl benzodithioate (>97%), $triethylamine_{abs}$ (>99.5%), furan (≥97%), furfuryl alcohol (98%), 3-aminopropanol (99%), 2-aminoethanol (≥99%), isopropenyl acetate (99%), methacryloyl chloride (97%), butyl methacrylate (BMA, 99%), ethyl 2-bromoisobutyrate (EBiB, 98%), 1,1,4,7,10,10-hexamethyltriethylenetetramine (HMTETA, 97%), maleic anhydride (98%), *n*-butylamine (99.5%), and anhydrous toluene were purchased from Sigma-Aldrich. 2-Isocyanotoethyl methacrylate (≥99%) was purchased from TCI Chemicals. Aluminum oxide 90 active neutral (70−230 mesh ASTM) was purchased from Merck Millipore. Na_2SO_3 (>98%) and 2,2′-azobis(2-methylpropionitrile) (AIBN, ≥98%) were purchased from Merck. The stabilizer of BMA was removed by passing it through active neutral alumina. AIBN was recrystallized from methanol. A stock solution containing 100 mg in 5 mL anhydrous toluene was prepared directly prior to use. CuBr was synthesized by reducing $CuBr_2$ with Na_2SO_3 in distilled water. The precipitating colorless solid was filtered, washed three times with ethanol, dried under vacuum, and stored under argon. All other chemicals were used as received. Synthetic procedures were performed under inert gas atmosphere applying Schlenk techniques.

Characterization. Fourier transform infrared (FTIR) spectroscopy measurements were performed applying a Bruker Vertex 70 spectrometer under ambient air (40 scans at a resolution of 4 cm^{-1}) in attenuated total reflectance (ATR) mode. Differential scanning calorimetry (DSC) measurements were carried out using a Netzsch DSC 204 F1 Phoenix with samples in aluminum crucibles with pierced lids and heated under nitrogen at a rate of 10 K/min. Solution NMR spectra were recorded with a Bruker Avance III HD 300/400 spectrometer at 25 °C (^1H at 300.13/400.13 MHz, ^{13}C at 75.48/100.61 MHz) using $CDCl_3$ as reference. The degree of substitution (dS) in polymers was determined using ^1H NMR integrals, where dS = (integral functional group) × 100/(integral OCH_2) [%]. Peak assignments of polymers can be found in the Supporting Information. Solid-state CP-MAS NMR spectra were recorded on a Bruker Avance 400WB spectrometer at 25 °C (^{13}C at 100.62 MHz, ^{29}Si at 79.50 MHz) and a contact time of 2.0 ms with a variable power contact time

DOI: 10.1021/acs.macromol.8b00601
Macromolecules XXXX, XXX, XXX−XXX

(ramp 10050). The rotor spin rate was 13 kHz, with delay time of 3–6 s. Adamantane was used as an external standard for ^{13}C NMR and octakis(trimethylsiloxy)silsesquioxane for ^{29}Si NMR. Elemental analysis was performed with a Leco 900 CHN analyzer. Films were compression-molded at 70 °C 24 h in a Teflon form (3 cm × 1 cm × 0.1 cm) which was held with a vice. Microscope images were recorded under polarized light using an Olympus BX60 microscope equipped with a Sony CCD-Iris color camera. Size exclusion chromatography (SEC) measurements in tetrahydrofuran (THF) were performed with a PSS (Polymers Standards Service) system, which included a Viscotek VE1121 pump, a Shodex refractive index detector, a PSS SLD 7000 multiangle light scattering detector, and styrene–divinylbenzene copolymer columns (PSS SDV) at a rate of 1 mL min^{-1}. A linear polystyrene standard was used for calibration, which causes deviations from expected molecular masses. UV–vis transmission spectra were recorded on a Lambda 750 instrument (PerkinElmer Inc., USA) equipped with a 100 mm integrating sphere from 500 to 248 nm with a 4 nm increment on 1 mm cuvettes with a drop-cast film of the sample. Rheological measurements were carried out on an Anton Paar Physica MCR 301 rheometer equipped with a CTD450 convection oven. Thin films (500 μm thick, 25 mm diameter) of the samples were compression-molded in a heatable press (Specac, 60 °C, 2 t, 1 min, baking paper for separation) and measured in oscillation mode using the PP25 measuring system with 25 mm plate diameter and a plate-to-plate distance of 0.5 mm. The measurements were conducted in the temperature range where the materials are present as a melt. The measurement starts at 70 °C; the temperature was increased to 120 °C, held for 1 h, and subsequently decreased to 70 °C. This temperature was held constant until the sample solidifies. STEM measurements were performed on a cold field emission gun TEM/STEM (JEOL JEM-ARM 200F) instrument, operated at an accelerating voltage of 200 kV and equipped with a STEM Cs corrector (CESCOR; CEOS GmbH Heidelberg). Images were obtained using a high angle annular bright-field (ABF) detector with a camera length of 8 cm. The sample was prepared by the ultramicrotomy technique with a thickness of about 20 nm and put on a copper grid coated with thin pure carbon holey film.

Synthesis. *3-Acetylaminopropanol (**1**).*[23] A mixture of isopropenyl acetate (25.97 g, 28.57 mL, 259.36 mmol) and 3-aminopropanol (5.0 g, 5.1 mL, 64.84 mmol) was heated at 60 °C for 3 h in a sealed vial. After the reaction was finished the residual isopropenyl acetate and acetone were distilled off under vacuum. The product was obtained as a yellow oil and used without further purification to synthesize **2**. Yield: 7.60 g (64.84 mmol, 100%). ^1H NMR (300 MHz, $CDCl_3$): δ 6.80 (s, 1H, H8 or H4), 4.12 (1H, H8 or H4), 3.58 (t, J = 5.7 Hz, 2H, H1), 3.32 (td, J = 6.0 Hz, 2H, H3), 1.93 (s, 3H, H7), 1.63 (quint, 2H, H2). ^{13}C NMR (75 MHz, $CDCl_3$): δ 171.64 (C5), 59.40 (C1), 36.56 (C3), 32.05 (C2), 23.03 (C7).

*3-Acetamidopropyl Methacrylate (**2**).* To a stirred solution of 3-acetylaminopropanol (**1**) (7.60 g, 64.84 mmol, 1.0 equiv) and triethylamine (7.87 g, 10.94 mL, 77.81 mmol, 1.2 equiv) in anhydrous CH_2Cl_2 (170 mL) a solution of methacryloyl chloride (8.13 g, 77.81 mmol, 1.2 equiv) in anhydrous CH_2Cl_2 (20 mL) was added dropwise at 0 °C. After complete addition, the mixture was allowed to warm to room temperature and stirred overnight. The orange slurry was concentrated to half of the volume, cooled to 0 °C, and filtered; the filtrate was extracted with water (2 × 25 mL). Afterward, the organic phase was separated, dried over $MgSO_4$, and concentrated *in vacuo*. The crude product was obtained as an orange oil. After purification via distillation *in vacuo* (132 °C, 7 × 10^{-3} mbar) pure **2** could be obtained as a colorless oil. Yield: 10.77 g (58.13 mmol, 90%). ^1H NMR (300 MHz, $CDCl_3$): δ 6.14–6.02 (m, J = 1.5, 1.0 Hz, 2H, H12, and H4), 5.58–5.50 (m, 1H, H12), 4.18 (t, J = 6.0 Hz, 2H, H1), 3.28 (td, J = 6.0 Hz, 2H, H3), 1.95 (s, 3H, H7), 1.92–1.90 (m, 3H, H13), 1.85 (quint, J = 6.0 Hz, 2H, H2). ^{13}C NMR (75 MHz, $CDCl_3$): δ 170.34 (C5), 167.65 (C9), 136.24 (C11), 125.83 (C12), 62.26 (C1), 36.47 (C3), 28.79 (C2), 23.31 (C7), 18.35 (C13). CHN_{theo} ($C_9H_{15}NO_3$): C, 58.36; H, 8.16; N, 7.56. CHN_{exp}: C, 57.68; H, 8.10; N, 7.22. IR: ν = 3290 ν(N–H), w; 3088 ν(N–H) w; 2960, 2931, 2871 (m, ν(C–H)); 1716 (s, ν(C=O)); 1639 (s, amide I ν(C=O)); 1551 (s, amide II ν(C–N) with contributions of δ(N–H)); 1443 (m, δ(C–H)); 1294 (s, ν(C–O–C)) cm^{-1}.

*2-(4-Butylureido)ethyl Methacrylate (**3**).* 2-Isocynatoethyl methacrylate (1 g, 6.44 mmol) was dissolved in absolute dichloromethane (30 mL), and *n*-butylamine (0.47 g, 0.64 mL, 6.44 mmol) was added dropwise. The colorless precipitate was filtered off and dried in vacuo. Yield: 1.47 g (6.44 mmol, 100%). ^1H NMR (400 MHz, $CDCl_3$): δ 6.19–6.07 (m, 1H, H1), 5.64–5.53 (m, 1H, H1), 4.68 (s, 1H, H9 or H11), 4.44 (s, 1H, H1, H9 or H11), 4.24 (t, J = 5.4 Hz, 2H, H6), 3.50 (q, J = 5.4 Hz, 2H, H8), 3.18–3.11 (m, 2H, H12), 1.94 (s, 3H, H4), 1.52–1.42 (m, 2H, H13), 1.41–1.27 (m, 2H, H15), 0.91 (t, J = 7.3 Hz, 3H, H16). ^{13}C NMR (75 MHz, $CDCl_3$): δ 167.73 (C5), 158.12 (C10), 136.22 (C2), 126.11 (C1), 64.37 (C6), 40.54 (C8), 39.88 (C12), 32.38 (C13), 20.15 (C4), 18.44 (C15), 13.89 (C16). CHN_{theo} ($C_{10}H_{11}NO_4$): C: 57.87; H: 8.83; N: 12.27. CHN_{exp}: C, 57.78; H, 8.57; N, 12.23. IR: ν = 3336 (w, ν(N–H)); 2964, 2931, 2858 (m, ν(C–H)); 1708 (s, ν(C=O)); 1618 (s, amide I ν(C=O)); 1574 (s, amide II ν(C–N) with contributions of δ(N–H)); 1446 (m, δ(C–H)); 1292 (s, ν(C–O–C)) cm^{-1}.

*2-(2-Hydroxyethyl)-3a,4,7,7a-Tetrahydro-1H-4,7-epoxyisoindole-1,3(2H)-dione (**4**).* A solution of 4,7,7a-tetrahydro-4,7-epoxyisobenzofuran-1,3-dione (10 g, 60.3 mmol) in methanol (250 mL) was purged with nitrogen for 10 min in an ice bath. Subsequently, ethanolamine (4 mL, 60.3 mmol) and triethylamine (6.10 g, 8.4 mL, 60.3 mmol) were added. The reaction mixture was allowed to warm up, and the temperature was increased to 70 °C for 20 h. Subsequently, ethanolamine (0.4 mL, 6.0 mmol) was added, and stirring was continued for 2 h at 70 °C. The solution turned pale yellow. After cooling to room temperature, the solution volume was reduced and stored at −18 °C. The precipitate was collected by vacuum filtration washed with isopropanol and used without further purification. Dissolving the solid in isopropanol and storing it at −18 °C leads to crystalline **4**. Yield: 10.72 g (51.25 mmol, 85%). ^1H NMR (300 MHz, $CDCl_3$): δ 6.53–6.48 (m, 2H, H1&2), 5.27 (t, J = 0.9 Hz, 2H, H3&6), 3.79–3.72 (m, 2H, H14), 3.71–3.63 (m, 2H, H13), 2.88 (s, 2H, H4&5), 2.37 (s, 1H, H15). ^{13}C NMR (75 MHz, $CDCl_3$): δ 176.92 (C7/9), 136.67 (C1/2), 81.15(C3/6), 60.57 (C14), 47.65 (C4/5), 41.97 (C13). CHN_{theo} ($C_{10}H_{11}NO_4$): C: 57.41; H: 5.30; N: 6.70. CHN_{exp} C: 57.85; H: 5.56; N 6.72.

Furfuryl methacrylate (FMA) (**5**)[24] and 2-(1,3-dioxo-3a,4,7,7a-tetrahydro-1*H*-4,7-epoxyisoindol-2(3*H*)-yl)ethyl methacrylate (MIMA, **6**)[25] were synthesized according to literature procedures. NMR and IR spectra can be found in SI2.

*General Procedure for the Synthesis of Copolymers **P1**–**P3** via ATRP.* BMA (100 equiv, 13.86 mL, 86.0 mmol), FMA (1.34 g) or MIMA (2.49 g) each 10 equiv (8.6 mmol), according to the polymer, and anhydrous toluene (54 mL) were mixed under an argon atmosphere. The mixture was degassed using four freeze–pump–thaw cycles. To the frozen mixture CuBr (1 equiv, 124 mg, 0.86 mmol) and HMTETA (1 equiv, 224 μL, 0.86 mmol) were added, and another two vacuum–argon cycles were performed. The reaction was carried out after addition of degassed EBiB (1 equiv, 126 μL, 0.86 mmol) by heating the mixture at 70 °C for 16 h. The polymers (listed in Table 1) were purified by passing the solution through an alumina column (active, neutral) to remove the catalyst. The polymers were precipitated from concentrated THF solution two times in ice-cold *n*-hexane and dried at room temperature under reduced pressure. Parts of the polymer samples were analyzed by SEC and ^1H NMR to determine the molar mass and molar mass distribution.

Table 1. Polymers Prepared via ATRP

	polymer	yield [%]	dS_F [%]	dS_M [%]	dS_H [%]	PDI
P1	pBMA	84	–	–	–	1.52
P2	FMAcoBMA	85	8.33	–	–	1.66
P3	MIMAcoBMA	60	–	–	6.0	2.40

P1. ^1H NMR (300 MHz, $CDCl_3$): δ 4.10–3.82 (m, 1H, OCH_2), 2.14–0.59 (m, 6H, pBMA backbone). IR: ν = 2958, 2931, 2874 (m,

DOI: 10.1021/acs.macromol.8b00601
Macromolecules XXXX, XXX, XXX–XXX

ν(C−H)); 1720 (s, ν(C═O)); 1460 (m, δ(C−H)); 1386 (m, $\delta(CH_3)$); 1242−1142 (s, ν(C−O−C)); 746 (m, $\rho((CH_2)_n)$) cm^{-1}.

P2. ^1H NMR (300 MHz, $CDCl_3$): δ 7.42 (s, 1H), 6.44−6.29 (m, 2H), 5.02−4.88 (m, 2H), 4.08−3.81 (m, 21H), 2.12−0.64 (m, 140H). IR: ν = 2958, 2931, 2874 (m, ν(C−H)); 1720 (s, ν(C═O)); 1460 (m, δ(C−H)); 1386 (m, $\delta(CH_3)$); 1242−1142 (s, ν(C−O−C)); 746 (m, $\rho((CH_2)_n)$) cm^{-1}.

P3. ^1H NMR (300 MHz, $CDCl_3$): δ 6.58−6.45 (m, 1H), 5.32−5.15 (m, 1H), 4.13−3.81 (m, 24H), 3.68−3.48 (m, 1H), 2.91−2.79 (m, 1H), 2.14−0.62 (m, 149H). **P3** deprotected: ^1H NMR (400 MHz, $CDCl_3$): δ 6.80−6.68 (m, 1H), 4.05−3.83 (m, 20H), 3.67−3.54 (m, 1H), 2.18−0.51 (m, 132H). IR: ν = 2958, 2931, 2874 (m, ν(C−H)); 1720 (s, ν(C═O)); 1460 (m, δ(C−H)); 1403 (m, δ(C−N)); 1386 (m, $\delta(CH_3)$); 1242−1142 (s, ν(C−O−C)); 746 (m, $\rho((CH_2)_n)$) cm^{-1}. **P3** deprotected: same signals +696 δ(maleimide) cm^{-1}.

*General Procedure for the Synthesis of Copolymers **P4**−**P6** via ARGET ATRP*. BMA (100 equiv, 13.86 mL, 86.0 mmol), a hydrogen bond forming monomer (H1 = 3-acetamidopropyl methacrylate (1.59 g) (**2**), H2 = 2-(3-butylureido)ethyl methacrylate (1.96 g) (**3**)), FMA (**5**) (1.34 g), MIMA (**6**) (2.49 g) (each 10 equiv, 8.6 mmol), and anhydrous toluene (54 mL) were mixed under an argon atmosphere. The mixture was degassed using four freeze−pump−thaw cycles. In the case of H2 (**3**) absolute methanol (3 mL) were added to ensure complete dissolution. To the frozen mixture CuBr (1 equiv, 124 mg, 0.86 mmol) and HMTETA (1 equiv, 224 μL, 0.86 mmol) were added, and another two vacuum−argon cycles were carried out. The reaction was carried out after addition of degassed EBiB (1 equiv, 126 μL, 0.86 mmol) by heating the mixture at 70 °C for 12 h. Because of the low conversion, fresh HMTETA (1 equiv, 224 μL) and $H_2NNH_2 \cdot H_2O$ (200 μL = 0.206 mg → 80% 0.165 mg = 3.29 μmol) were added to the reaction mixture, and stirring was continued for another 12 h at 70 °C. The polymers (listed in Table 2) were purified by passing the solution through an alumina column (active, neutral) to remove the catalyst. The polymers were precipitated from concentrated THF solution two times in ice-cold *n*-hexane and dried at room temperature under reduced pressure. Parts of the polymer samples were analyzed by SEC and ^1H NMR to determine the molar mass, molar mass distribution, and dS.

Table 2. Polymers Prepared via ARGET ATRP

	polymer	yield [%]	dS_F [%]	dS_M [%]	dS_H [%]	PDI
P4	BMAcoH1	69	–	–	–	1.60
P5	FMAcoMIMAcoBMAcoH1 = $EKH1_A$	75	7.5	6.6	7.0	3.25
P6	FMAcoMIMAcoBMAcoH2 = $EKH2_A$	62	7.0	4.3	9.9	2.07

P4. ^1H NMR (300 MHz, $CDCl_3$): δ 4.08−3.85 (m, 15H), 3.44−3.25 (m, 1H), 2.11−0.63 (m, 100H). IR: ν = 3396 (w, ν(N−H)); 2958, 2931, 2874 (m, ν(C−H)); 1720 (s, ν(C═O)); 1460 (m, δ(C−H)); 1533 (m, ν(C−N) and δ(N−H)); 1388 (m, ν(C−N)), 1386 (m, $\delta(CH_3)$); 1242−1142 (s, ν(C−O−C)); 746 (s, $\rho((CH_2)_n)$) cm^{-1}.

P5. ^1H NMR (400 MHz, $CDCl_3$): δ 7.51−7.34 (m, 1H), 6.64−6.48 (m, 2H), 6.48−6.29 (m, *J* = 19.8 Hz, 2H), 5.34−5.18 (m, 1H), 5.06−4.88 (m, 1H), 4.19−3.83 (m, 22H), 3.83−3.68 (m, 2H), 3.48−3.24 (m, 2H), 3.10−2.86 (m, 1H), 2.33−0.48 (m, 163H). IR: ν = 3396 (w, ν(N−H)), 2958, 2931, 2874 (m, ν(C−H)); 1720 (s, ν(C═O)); 1460 (m, δ(C−H)), 1525 (m, ν(C−N) and δ(N−H)); 1392 (m, ν(C−N)), 1386 (m, $\delta(CH_3)$); 1242−1142 (s, ν(C−O−C)); 746 (m, $\rho((CH_2)_n)$) cm^{-1}.

P6. ^1H NMR (400 MHz, $CDCl_3$): δ 7.40 (s, 1H), 6.51 (d, *J* = 16.7 Hz, 1H), 6.34 (d, *J* = 20.6 Hz, 2H), 5.26 (s, 2H), 4.94 (s, 2H), 3.91 (s, 22H), 3.78 (dd, *J* = 14.9, 9.6 Hz, 2H), 3.50 (s, 2H), 3.17 (s, 2H), 2.96 (s, 1H), 2.03−1.69 (m, 21H), 1.69−1.50 (m, 23H), 1.51−1.28 (m, 27H), 1.27−0.57 (m, 73H). IR: ν = 3400 (w, ν(N−H)); 2958, 2931, 2874 (m, ν(C−H)); 1720 (s, ν(C═O)); 1637 (m, amide I ν(C═O)); 1558 (m, amide II ν(C−N) with contributions of δ(N−H)); 1460 (m, δ(C−H)); 1392 (m, (ν(C−N−C), δ(N−H) and $\delta(CH_3)$)); 1242−1142 (s, ν(C−O−C)); 746 (m, $\rho((CH_2)_n)$) cm^{-1}.

*General Procedure for the Synthesis of Copolymers **P7**−**P10** via RAFT*. BMA (10 equiv, 1.39 mL, 8.6 mmol), a hydrogen bond forming monomer (H1 = 3-acetamidopropyl methacrylate (159 mg) (**2**), H2 = 2-(3-butylureido)ethyl methacrylate (196 mg) (**3**)), 2-isocyanatoethyl methacrylate (133 mg), FMA (**5**) (134 mg), MIMA (**6**) (249 mg) (each 1 equiv, 0.86 mmol), and anhydrous toluene (5.4 mL) were mixed under an argon atmosphere. In the case of H2 (**3**) absolute methanol (0.3 mL) was added to ensure complete dissolution. The mixture was degassed using four freeze−pump−thaw cycles. To the frozen mixture 2-cyanopropan-2-yl benzodithioate (19 mg, 0.086 mmol) and AIBN (10 mg, 0.061 mmol in 0.5 mL of toluene (abs) from stock solution, previously degassed) were added, and two more freeze−pump−thaw cycles were carried out. The reaction mixture was stirred at 70 °C for 20 h. In the case of the 2-isocyanatoethyl methacrylate modified polymer (**P10**), *n*-butylamine (55 mg, 0.086 mmol) was added to the reaction mixture after cooling to room temperature, and stirring was continued for another 12 h. The polymers (listed in Table 3) were purified by precipitation in ice-cold *n*-hexane and dried at room temperature under reduced pressure. Parts of the polymer samples were analyzed by SEC and ^1H NMR to determine the molar mass and molar mass distribution.

P7. ^1H NMR (400 MHz, $CDCl_3$): δ 7.49−7.33 (m, 1H), 6.62−6.46 (m, 2H), 6.46−6.28 (m, *J* = 21.6 Hz, 2H), 5.35−5.24 (m, *J* = 10.8 Hz, 2H), 5.09−4.87 (m, 2H), 4.09−3.83 (m, 21H), 3.83−3.66 (m, *J* = 6.7 Hz, 3H), 3.04−2.90 (m, 1H), 2.78−2.60 (m, 2H), 2.13−0.55 (m, 153H). IR: ν = 3403 (w, ν(N−H)); 2958, 2931, 2874 (m, ν(C−H)); 1720 (s, ν(C═O)); 1460 (m, δ(C−H)); 1535 (m, ν(C−N) and δ(N−H)); 1388 (m, ν(C−N)); 1386 (m, $\delta(CH_3)$); 1242−1142 (s, ν(C−O−C)); 746 (m, $\rho((CH_2)_n)$) cm^{-1}. **P7** deprotected: same signals +696 δ(maleimide) cm^{-1}.

P8. ^1H NMR (400 MHz, $CDCl_3$): δ 7.49−7.33 (m, 1H), 6.62−6.46 (m, 2H), 6.46−6.28 (m, *J* = 21.6 Hz, 2H), 5.35−5.24 (m, *J* = 10.8 Hz, 2H), 5.09−4.87 (m, 2H), 4.09−3.83 (m, 21H), 3.83−3.66 (m, *J* = 6.7 Hz, 3H), 3.04−2.90 (m, 1H), 2.78−2.60 (m, 2H), 2.13−0.55 (m, 153H). IR: ν = 3400 (w, ν(N−H)); 2958, 2931, 2874 (m, ν(C−H)); 1720 (s, ν(C═O)); 1637 (m, amide I ν(C═O); 1558 (m, amide II ν(C−N) with contributions of δ(N−H)); 1460 (m, δ(C−H)); 1392 (m, ν(C−N−C), δ(N−H) and $\delta(CH_3)$); 1242−1142 (s, ν(C−O−C)); 746 (m, $\rho((CH_2)_n)$) cm^{-1}.

P9. ^1H NMR (400 MHz, $CDCl_3$): δ 7.47−7.32 (m, 1H), 6.59−6.47 (m, 1H), 6.44−6.28 (m, 2H), 5.31−5.22 (m, 1H), 5.05−4.86 (m, 2H), 4.11−3.83 (m, *J* = 58.4 Hz, 19H), 3.81−3.68 (m, 2H), 3.55 (dd, *J* = 10.5, 5.4 Hz, 2H), 3.04−2.89 (m, 1H), 2.09−1.70 (m, 20H), 1.70−1.49 (m, 22H), 1.51−1.29 (m, 21H), 1.29−0.67 (m, 61H). IR: ν = 2958, 2931, 2874 (m, ν(C−H)); 2270 (m, ν(OCN)); 1720 (s, ν(C═O)); 1460 (m, δ(C−H)); 1386 (m, $\delta(CH_3)$); 1242−1142 (s, ν(C−O−C)); 746 (m, $\rho((CH_2)_n)$) cm^{-1}.

Table 3. Polymers Prepared via RAFT

	polymer	yield [%]	dS_F [%]	dS_M [%]	dS_H [%]	PDI
P7	FMAcoMIMAcoBMAcoH1 = $EKH1_R$	68	8.6	6.4	5.6	5.51
P8	FMAcoMIMAcoBMAcoH2 = $EKH2_R$	79	8.7	6.5	9.8	2.76
P9	FMAcoMIMAcoBMAcoOCN = $EKOCN_R$	–	9.1	5.9	9.6	–
P10	$EK(OCN+amine)_R$ = $EKH2_R$	84	7.8	5.9	9.4	3.48

DOI: 10.1021/acs.macromol.8b00601
Macromolecules XXXX, XXX, XXX−XXX

Table 4. Composition of Polymers P1−P10

		W	X	Y	Z	M_n theor [g/mol]	M_n ^{1}H NMR [g/mol]	M_n SEC [g/mol]	PDI SEC	T_g ($^1/_2\Delta c_p$) [°C]
P1	pBMA	–	–	–	n	14200	13100	17200	1.52	29
P2	pBMAcoFMA	–	1n	–	10n	15900	14800	21800	1.66	26
P3	pBMAcoMiMA	1n	–	–	10n	17000	15800	11800	2.40	30
P4	pBMAcoH1	–	–	1n	10n	16100	15600	19200	1.60	34
P5	$EKH1_A$	1n	1n	1n	10n	20900	17800	16500	3.25	63
P6	$EKH2_A$	1n	1n	1n	10n	21300	16800	20300	2.07	63
P7	$EKH1_R$	1n	1n	1n	10n	20900	16500	9070	5.51	53
P8	$EKH2_R$	1n	1n	1n	10n	21300	19400	17000	2.76	53
P9	$EK(OCN)_R$	1n	1n	1n	10n	20600	18500	–	–	63
P10	$EK(OCN+amine)_R$	1n	1n	1n	10n	21300	postmod	18000	3.48	61

P10. ^{1}H NMR (400 MHz, $CDCl_3$): δ 7.42 (s, 1H), 6.59−6.50 (m, 1H), 6.45−6.31 (m, 2H), 5.32−5.22 (m, 2H), 5.04−4.89 (m, 2H), 4.12−3.84 (m, 22H), 3.86−3.70 (m, 3H), 3.63−3.41 (m, 2H), 3.27−3.12 (m, 2H), 3.06−2.90 (m, 1H), 2.10−1.71 (m, 22H), 1.71−1.53 (m, 29H), 1.53−1.30 (m, 28H), 1.30−0.55 (m, 74H). IR: ν = 3400 (w, ν(N−H)); 2958, 2931, 2874 (m, ν(C−H)); 1720 (s, ν(C═O)); 1637 (m, amide I ν(C═O)); 1558 (m, amide II ν(C−N) with contributions of δ(N−H)); 1460 (m, δ(C−H)); 1392 (m, ν(C−N−C), δ(N−H) and $\delta(CH_3)$); 1242−1142 (s, ν(C−O−C)); 746 (m, $\rho((CH_2)_n)$) cm^{-1}.

Synthesis of Octafunctional Hydrogen Bond Bearing Spherosilicate.[22] Tetraethyl orthosilicate was condensed with tetramethylammonium pentahydrate to an SiO_2 octaanion, which was transferred to the Si−H terminated cube by conversion with dimethylchlorosilane.[26,27] Hydrosilylation with ω-bromoalkenes resulted in cubes, which could be further converted with NaN_3 to the corresponding azides. After catalytic reduction to the amine, the highly reactive cube could be converted with propyl isocyanate to the desired hydrogen bond bearing spherosilicate.[22]

Synthesis of Composites (C1−C5). The hybrid materials **C1**−**C5** (Scheme 2 and Table 4) were synthesized by mixing (a) **P1** with **C6U** = **C1** (control) with OctaUreaPOSS (**C6U**), (b) **P1**, **P2**, and **P3** with **C6U** = **C2**, (c) **P2**, **P3**, and **P4** with **C6U** = **C3**, (d) one-component polymer $\mathbf{EKH1_A}$ = (**P5**) with **C6U** = **C4**, and (e) one-component polymer $\mathbf{EKH2_R}$ = (**P6**) with **C6U** = **C5**. The polymers or polymer mixtures (500 mg in total, 167 mg each) were dissolved in THF (5 mL) and **C6U** (125 mg, M_w = 2478.20 g/mol, 0.05 mmol) in methanol (10 mL). After mixing, the solvents were evaporated at room temperature in a vacuum, and the respective precipitated solid was pressed into a Teflon mold. The deprotection of maleimide in MIMA (**6**) containing hybrid materials (**C2**−**C5**) was performed in the bulk material for 30 min at 120 °C. Cross-linking was realized by heating the samples at 70 °C for 20 h.

3. RESULTS AND DISCUSSION

Synthesis and Characterization of Polymers P1−P10. Polymers containing DA as well as hydrogen donor and acceptor functions were synthesized via controlled radical polymerization (CRP), in particular ATRP, ARGET ATRP, or RAFT. In the present work, we decided to locate the diene as well as the dieonophile in the polymer matrix to ascertain a high degree of freedom of these chemical reaction partners. Applying this approach, it can be guaranteed that the maleimide and furan functional groups are statistical distributed and therefore equal in their availability to undergo DA reaction.[10] As a second reversible network, we introduced amide and urea motifs as supramolecular units because of their ability to form hydrogen bonds. The precursors are commercially available and the monomers can be produced in one or two reaction steps. Hydrogen bonds equilibrate at room temperature after damage and according to that a reconnection of cut interfaces at or below nanometer scale is immediately possible to ensure the proximity of DA moieties. Scheme 1 and Table 4 summarize the synthesized polymers.

Scheme 1. Statistical Copolymers P1−P10

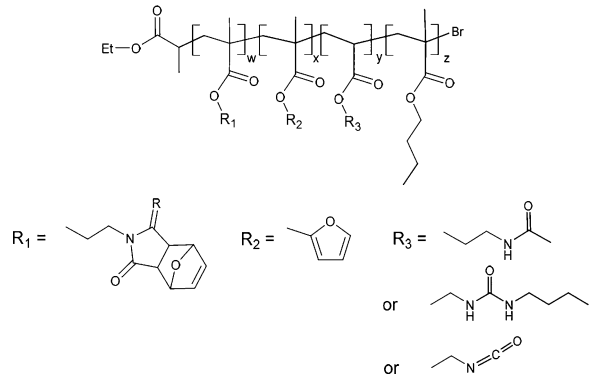

All macromolecules were statistic copolymers from butyl methacrylate, furfuryl methacrylate (**5** = R_2), protected maleimidoethyl methacrylate (**6** = R_1), and a hydrogen bond building moiety, namely 3-acetamidopropyl methacrylate (**2** = R_3), 2-(4-butylureido)ethyl methacrylate (**3** = R_3), or 2-isocyanatoethyl methacrylate (R_3) as functional monomers (Scheme 1 and Table 4). The protection of maleimide is necessary because otherwise cross-linking with the reactive maleimide double bond would occur.[8] The main component within the polymer is butyl methacrylate (70−90 equiv), and each functional monomer was applied in 10 equiv.

P1−**P3** containing only BMA, FMA, and protected MIMA could be polymerized similar to literature known procedures applying a Cu(I)-catalyzed ATRP using HMTEA as a ligand.[8,28] When hydrogen bond donors, particulary nitrogen donors, were added to the mixture, only very little conversion was observed. Literature procedures describe the polymerization of 3-acetamidopropyl methacrylate (**2** = R_3 = H1) applying an ATRP with CuBr PMDETA catalyst in DMF.[29] In our systems, the polymerization remained quite incomplete. Trying to polymerize hydrogen bond bearing 2-(4-butylureido)ethyl methacrylate (**3** = R_3 = H2) under the same conditions, almost no conversion was obtained after 16 h. Adjusting the reaction conditions to an ARGET ATRP like polymerization instead, even the strong donating monomers could be polymerized in high quantity (up to 90%). [CuBr(HMTETA)]Br seems to be not stable long enough under the given reaction conditions. Therefore, hydrazine hydrate was applied as reducing agent. In addition, fresh ligand was added after 12 h, and the desired products (**P4**−**P6**) could be synthesized in up to 95% conversion (as determined by ^{1}H

DOI: 10.1021/acs.macromol.8b00601
Macromolecules XXXX, XXX, XXX−XXX

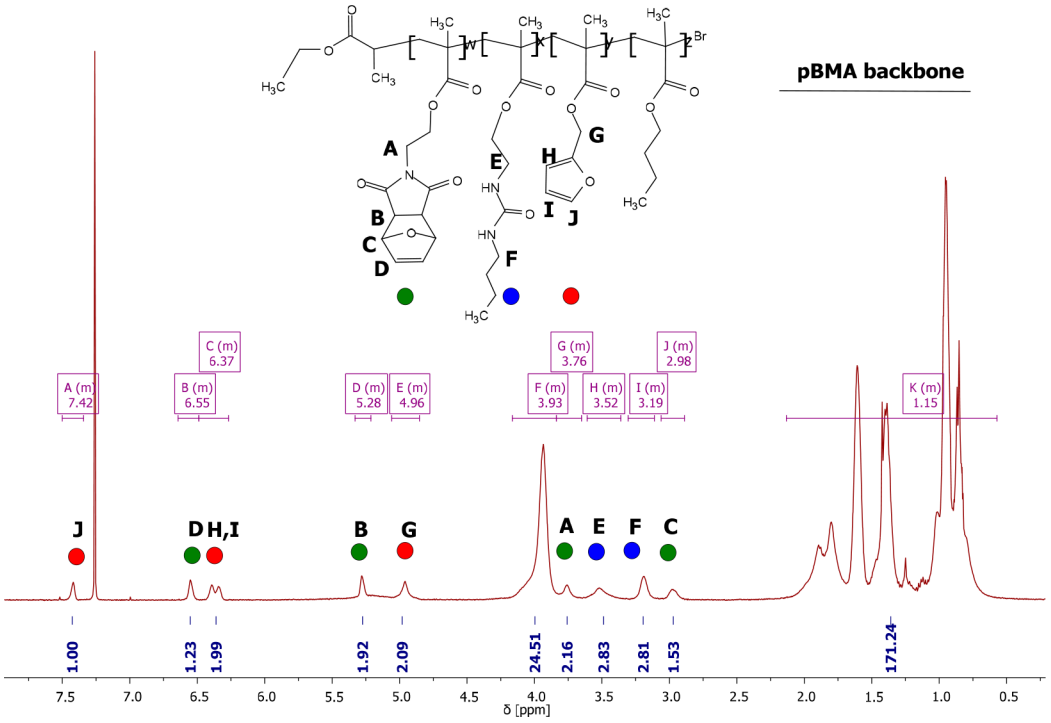

Figure 1. ^{1}H NMR of one-component polymer EKH2$_A$ = **P6**.

NMR). SEC measurements revealed a rather broad mass distribution (PDI = 1.52−2.40). The highest value was obtained for maleimide containing **P3**, presumably because of impurities of small amounts of deprotected maleimide, which can undergo irreversible cross-linking.[8] The obtained one-component polymers are soluble in common organic solvents such as acetone, $CHCl_3$, or THF.

As an alternative route a reversible addition−fragmentation chain transfer (RAFT) polymerization was applied because it tolerates more functional groups than ATRP and requires no metal catalyst. Using 2-cyanopropan-2-yl benzodithioate as RAFT agent and AIBN as initiator, the hydrogen bond bearing monomers could be incorporated without difficulties within the polymer. As the urea bearing monomer (**3**) is insoluble in toluene, a small amount of methanol had to be added to the mixture. To keep the reaction parameters more similar to the polymerization of EKH1$_A$ (**P5**) and EKH1$_R$ (**P7**), the polymerization of the 2-isocyanotoethyl methacrylate was also investigated. The successful polymerizations of isocyanates in RAFT have been described before.[30,31] In a post-modification, the crude polymer could be directly converted with *n*-butylamine to the desired EKH2$_R$ (**P10**). Conversions of 79−91% were obtained, and molar mass distributions from PDI = 2.76−5.51 were determined.

^{1}H NMR spectra were used to verify that there are no unreacted monomers left after work-up. The degree of substitution was determined by setting the integral of all OCH_2 signals (at 3.93 and 4.96 ppm), which represents the complete polymer backbone, in relation to one proton of each functional comonomer. SEC measurements revealed that the PDIs are between 1.5 and 5.5. The reason for these relatively broad molar mass distributions, in particular, when maleimide participates within the reaction, is mentioned above. However, the obtained polymer chains are still soluble and linear and have low molecular weights (below 22000 g/mol). The desired functional monomers were incorporated in a good substitution degree (dS = 4.3−9.9%).

Figure 1 displays the ^{1}H NMR of one-component polymer EKH2$_A$ = **P6**. The red dots at 7.42, 6.37, and 4.96 ppm indicate protons belonging to the furan moiety, the green dots at 6.55, 5.28, 3.76, and 2.98 ppm show the signals of protected maleimide group, and the blue dots at 3.52 and 3.19 ppm show the CH_2N groups of copolymerized urea derivative. After ARGET ATRP, furan was found in 7.0%, protected maleimide in 4.3%, and 2-(4-butylureido)ethyl methacrylate (**3** = H2) in 9.9% for EKH2$_A$ = **P6**. By use of RAFT polymerization for EKH2$_R$ = **P8**, a substitution degree of 8.7% for furan, 6.5% protected maleimide, and 9.8% for **3** (H2) was observed. ^{1}H NMR spectra and degree of substitution of all other polymers can be found in the Supporting Information.

By comparison of the IR spectra of functional polymers with the pure pBMA polymer **P1**, the incorporation of functional groups could be further verified (Figure 2). Pure pBMA shows similar bands like PMMA: 2958−2874 cm^{-1} C−H stretching, 1720 cm^{-1} C═O stretching, 1460 cm^{-1} C−H bending, 1386 and 746 cm^{-1} α-CH_3-vibration, 1242−1142 cm^{-1} C−O−C stretching. The functional polymer shows additional peaks, which are typical for the urea structure motive. At 3400 cm^{-1} the N−H stretching vibration, at 1637 cm^{-1} amide I (C═O stretching), 1558 cm^{-1} amide II bands (C−N stretching with contributions of N−H bending), and 1392 cm^{-1} (C−N−C stretching, N−H deformation and CH_3 deformation).[32,33] The H2 monomer (**3**) shows the corresponding peaks at 3336, 1620, 1574, and 1382 cm^{-1}. Further IR spectra can be found in the Supporting Information.

Analysis of Polymers via DSC. All polymers were analyzed using DSC by cooling the samples to −25 °C and heating to 200 °C twice. The presence of only one T_g in all polymers evidences an ideal miscibility and a homogeneous, statistical distribution of of each comonomer (Table 4 and Figure 3).[34]

DOI: 10.1021/acs.macromol.8b00601
Macromolecules XXXX, XXX, XXX−XXX

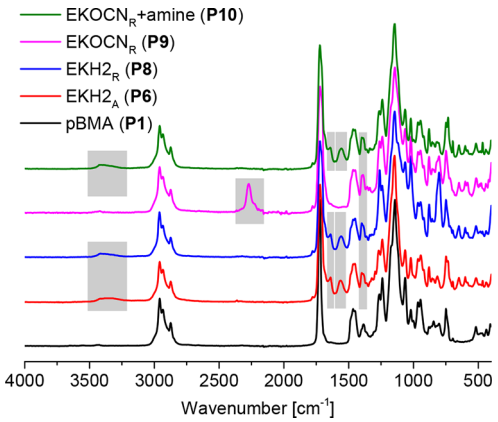

Figure 2. Comparison of IR spectra of pure pBMA with functional one-component polymers EKH_2.

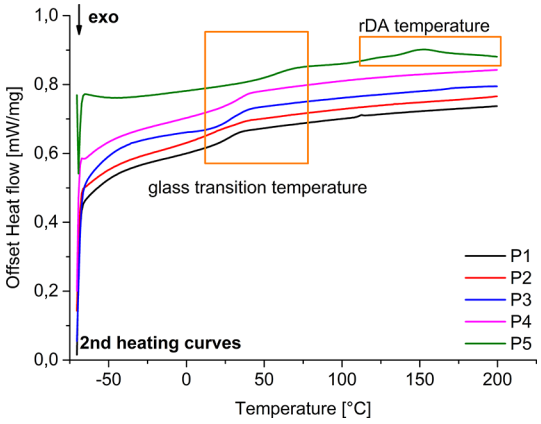

Figure 3. DSC measurements of second heating curve to determine the glass transition temperature from **P1**−**P5**.

The T_g is a function of molecular weight, amount, chemical nature of side chains, the thermal history of a polymer, and the cross-linking between the single chains. In polymers containing the maximum number of two comonomers (**P1**−**P4**) the glass transition is significantly lower with 26−34 °C, while in one-component polymers consisting of four comonomers (**P5**−**P12**) the T_g's are between 53 and 63 °C. The T_g's were analyzed using the second heating curve, in which cross-linking of single polymer chains already took place to a certain amount. Consequently, the T_g's of **P5**−**P12** are about 20−30 °C higher than those of **P1**−**P4** (Table 4). A second effect should be the hydrogen bond forming side chains on a hydrogen bond forming spine, which makes an interlock more probable and thus leads also to an increased T_g. All protected maleimide-containing polymers (**P3**, **P5**−**P10**) show a broad endothermic signal between 100 and 200 °C belonging to the rDA reaction in the first heating cycle, which corresponds to the deprotection of maleimide and evaporation of furan (compare Figure 5). DSC curves of other polymers (**P6**−**P10**) are displayed in the Supporting Information (Figure S28).

FTIR spectra (Figure 4) show the appearance of maleimide deformation band after deprotection of the polymer **P5** in bulk. This observation further confirms that after synthesis all maleimide moieties are still protected. After heating to 120 °C for 30 min, a small and sharp signal at 696 cm^{-1} for ring deformation can be detected, which indicates free, unprotected, and intact maleimide.

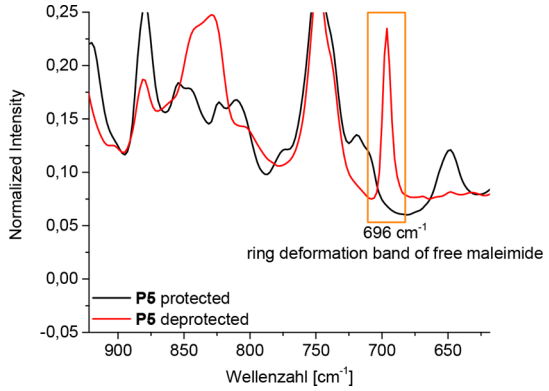

Figure 4. Observation of maleimide deformation band as indicator for successful deprotection of polymer **P5**.

The DSC curve in Figure 5 shows the deprotection of $EKH2_R$ (**P8**) in the first heating cycle, which causes the high

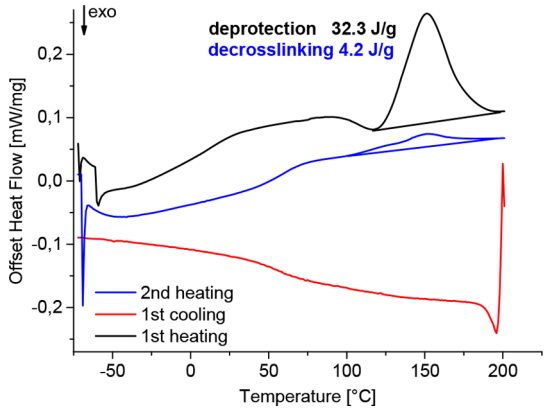

Figure 5. DA/rDA cycles of **P8** = $EKH2_R$.

endothermic signal (32.3 J/g) between 120 and 200 °C. Because of the evaporation energy of furan, the signal is much higher than the one in the second heating cycle. During the measurement, the sample passes the DA temperature and thus parts of the one-component polymer cross-link. Upon the second heating to rDA temperature, the de-cross-linking causes an endothermic signal (4.2 J/g).

The FTIR and DSC measurements show the efficient reversibility of synthesized one-component polymer **P9**.

Synthesis of Composites. Hybrid materials (Scheme 2 and Table 5) were synthesized by mixing (a) **P1** with OctaUreaPOSS (**C6U**) = **C1** (control), (b) **P1**, **P2**, and **P3** with **C6U** = **C2**, (c) **P2**, **P3**, and **P4** with **C6U** = **C3**, (d) one-component polymer $EKH1_A$ = **P5** with **C6U** = **C4**, and (e) one-component polymer $EKH2_R$ = **P8** with **C6U** = **C5** in an appropriate solvent mixture. **C1** is the pure nonfunctional pBMA mixed with the filler as a control experiment. **C2** also misses hydrogen bonds within the matrix but has the DA moieties for covalent cross-linking. **C3** is a mixture of all desired functions, but each is located in its own polymer. **C4** is the one-component matrix bearing amide and **C5** the one that is bearing urea groups in the backbone. By investigation of these different compositions, the contributions of the single forces should be judged.

For a good solubility the polymers were dissolved in THF and **C6U** in methanol. After mixing, the solvents were

DOI: 10.1021/acs.macromol.8b00601
Macromolecules XXXX, XXX, XXX−XXX

Scheme 2. General Procedure for Synthesis of Hybrid Materials: (1) Dissolve and Mix Components in THF/Methanol (20 wt % C6U); (2) Evaporate Solvent; (3) Placing Solid Mixture in Teflon Mold, Heating Sample at 120 °C, 30 min (Deprotection) and 70 °C, 20 h (Cross-Linking)

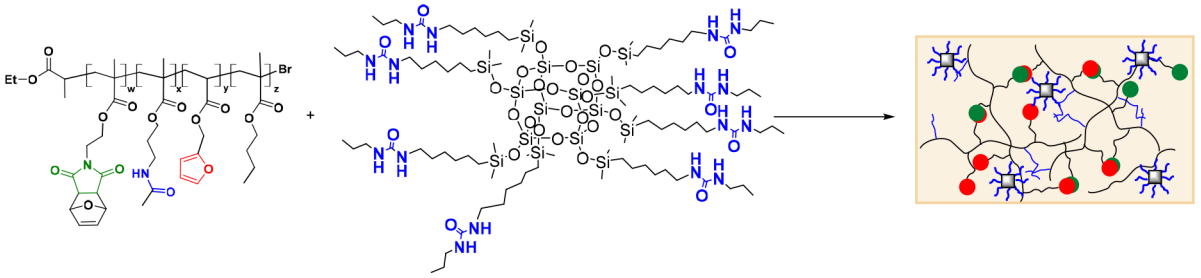

Table 5. Synthesized Composites and Their Abbreviations

	organic matrix	inorganic filler
C1	pBMA	each hybrid material contains 20 wt % **C6U** cube
C2	pBMA + pBMAcoFMA + pBMAcoMIMA	
C3	pBMAcoFMA + pBMAcoMIMA + pBMAcoH1	
C4	$EKH1_A$	
C5	$EKH2_R$	

evaporated at room temperature in a vacuum and the respective precipitated solid was pressed into a Teflon mold.

In Figure 6, the resulting hybrid material specimens with 1 mm thickness and edge length of 1 cm × 1 cm of **C1**, **C2**, **C3**, and **C5** are shown. In **C1** and **C2** a macroscopically visible inhomogeneous distribution was found, although the solvent was evaporated during stirring, while **C3**, **C4**, and **C5** show a uniform material (Figure 6).

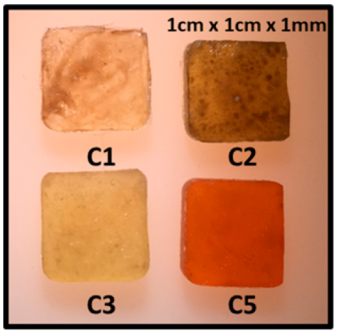

Figure 6. Images of hybrid materials **C1**, **C2**, **C3**, and **C5**.

The deprotection of maleimide in MIMA (**6**) containing hybrid materials (**C2**–**C5**) was performed by heating the bulk material to 120 °C for 30 min. Subsequently, the materials were cross-linked by heating the specimens at 70 °C for 20 h.

Reversibility of DA Reaction in Hybrid Materials. FTIR measurements (Figure 7) confirm the incorporation of **C6U** by the appearance of typical Si–O–Si bonds and the cage deformation vibration at 557 cm^{-1}. The position of the N–H vibration can be seen as an indicator that hydrogen bonds are formed. In dilute solutions, the signals for the urea N–H bond is typically observed around 3400 cm^{-1}, which means no hydrogen bonds are formed. In bulk, the lower wavenumber of 3300 cm^{-1} indicates hydrogen bonds within the hybrid material.[32,33] The presence of only one N–H vibration at 3336 cm^{-1} indicates the formation of a dynamic hydrogen bond network, formed between filler and matrix. Further IR spectra of composites are shown in Figure S29.

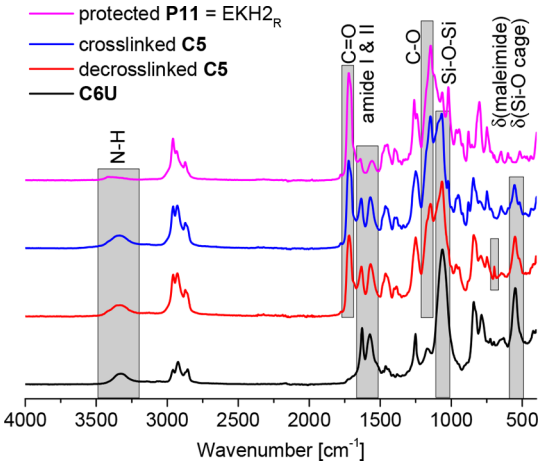

Figure 7. IR spectra of **P11** and **C6U** = **C5**.

Although the absorbance of urea groups (0.4 mmol in 125 mg of **C6U**) cause strong vibrations, the typical maleimide (maximum 0.24 mmol in 500 mg of **P5**) deformation vibration at 696 cm^{-1} becomes visible after deprotection of the hybrid material in bulk. After cross-linking at 70 °C for 20 h, this vibration disappears again, which indicates cross-linking within the material.

DSC measurements from −25 to 200 °C with a heating rate of 10 K/min were used to visualize DA cycles by thermal treatment of the composites. Although temperatures up to 200 °C could lead to polymerization and decomposition of maleimides in the sample, this temperature program was chosen to display the whole energy consumption of rDA reaction. For the one-component cross-linked composite **C5**, the first heating cycle show a broad endothermic signal from 100 to 200 °C of 18.5 J/g (Figure 8).

The T_g signal is located around 53 °C, like in the initial polymer, but it should be considered that the signal may have contributions from the DA reaction. After the first deprotection within DSC measurement, the sample is maximum 22 min in the DA temperature range, which is quite a short time to reconnect for the DA groups compared to the normally applied 20 h in bulk. However, the appearance of the rDA signal with 3.1 J/g in the second heating cycle shows that cross-linking took place. Directly after that, the sample was heated isothermal at 70 °C for 20 h in DSC (Figure 8, third heating). This heating represents the experimental conditions, like they are applied for the bulk material. A signal of 4.4 J/g

DOI: 10.1021/acs.macromol.8b00601
Macromolecules XXXX, XXX, XXX–XXX

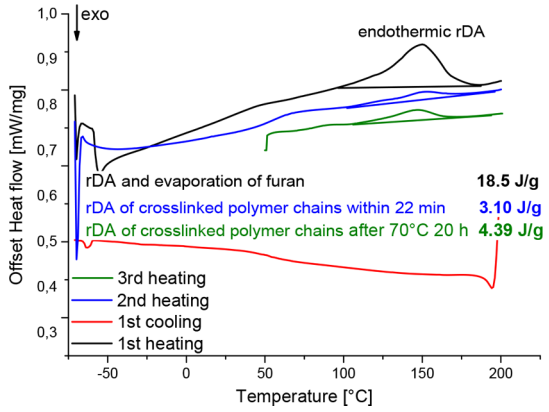

Figure 8. DA/rDA cycles of **C5**.

which is 15% higher was observed compared to the short cross-linking time of 22 min in DSC.

The DSC measurements display a good reversibility of DA reactions in this hybrid material. Situating the DA functional groups only within the matrix polymers seems to be advantageous compared to systems where the groups are located on inorganic surfaces.[10] Even with a high filler content of 20 wt % the spherosilicate does not limit the DA reaction, as can be concluded from the rDA signal after cross-linking of **C5**. The hybrid material shows a signal of 3.1, and the pure polymer $EKH2_R$ (**P8**, Figure 5) shows a signal of 4.2 J/g after short cross-linking time of 22 min.

Self-Healing Studies. ^{13}C CP MAS NMR measurements were conducted to follow the cross-linking ability of the produced materials. The measurements were performed on protected **P5** and cross-linked **C4** (Figure 9).

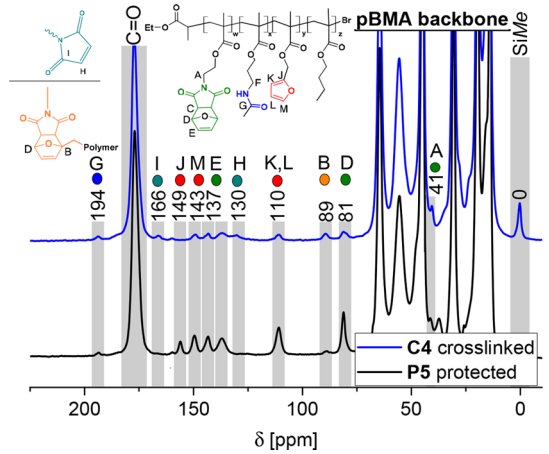

Figure 9. ^{13}C CP-MAS NMR spectra of protected **P5** and cross-linked composite **C4**.

In ^{13}C CP-MAS NMR, the ratio of signals that belong to DA/rDA can be visualized. The colored dots in Figure 9 indicate the relevant peaks, which are the signals of the CH_2 group next to maleimide nitrogen at 41 ppm, the bridgehead carbons of the C−O−C motive in the DA product at 81 and 89 ppm, and the double bond of the DA adduct at 137 ppm. After deprotection the signals at 130 and 166 ppm of free maleimide became visible. The signals at 110, 143, and 149 ppm belong to the four carbon atom signals of the furan ring and at 194 ppm the characteristic signals for the C═O group of the imide can be observed. The successful incorporation of spherosilicates is indicated by the signal of $Si-CH_3$ groups at 0 ppm. ^{29}Si CP-MAS NMR spectra of composite **C4** evidence that the silica framework remains intact and in its original high symmetry, as indicated by only two sharp signals: −11.99 ppm ($OSi(CH_3)_2R$) and −109.21 ppm (SiOSi) (Figure 10). This spectrum is in good agreement with solution ^{29}Si NMR of the pure compound **C6U**.

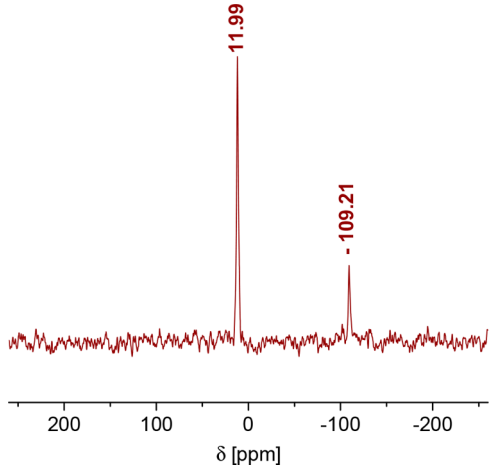

Figure 10. ^{29}Si CP-MAS of cross-linked composite **C4**.

UV-vis measurements were performed to follow the DA reaction as a function of temperature within 24 h (Figure 11).

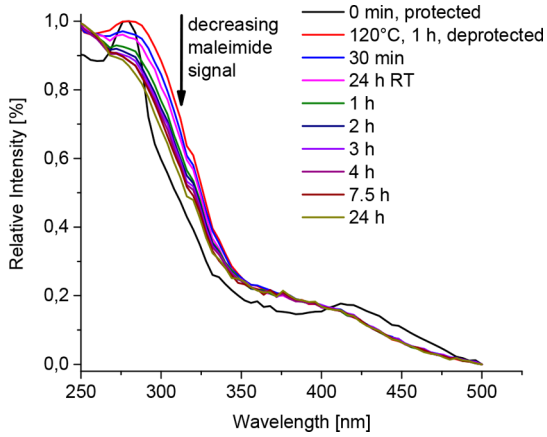

Figure 11. UV-vis spectra followed over time during the cross-linking reaction of **C4** at 70 °C.

A comparison of the free maleimide UV-vis absorption around 284 nm was used to plot the conversion over time (Figure 12). Cross-linking proceeds mostly within the first 4 h. A conversion of 80% was reached already within this short period in the pure polymer **P8** (Figures S37−39) as well as in the hybrid material (**C4**). These results show that the reactivity of the one-component polymer is not decreased by the addition of **C6U**.

Rheological measurements of pure polymer **P8** and hybrid material **C4** were conducted. The storage modulus was observed over time while the temperature was varied from 70 °C (protected maleimide) to 120 °C for 1 h (deprotection) and back to 70 °C (cross-linking). In the pure polymer (Figure S41), an increasing storage modulus was observed after

DOI: 10.1021/acs.macromol.8b00601
Macromolecules XXXX, XXX, XXX−XXX

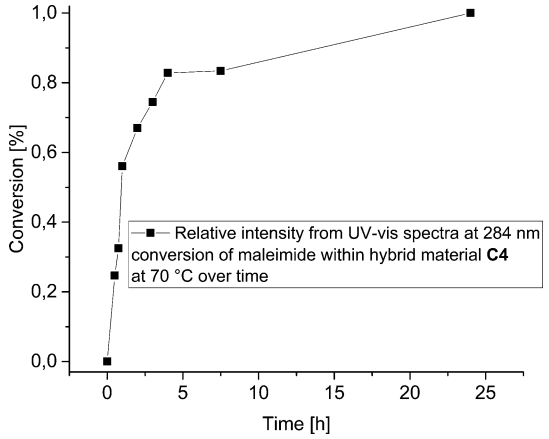

Figure 12. DA conversion over time of **C4** determined from UV-vis spectra.

deprotection, upon cooling to the cross-linking temperature of 70 °C. After approximately 1 h at 70 °C, the polymer melt solidifies, and the observation of storage modulus was no longer possible. The increasing modulus as well as turning from polymer melt to a solid already at 70 °C indicates a successful DA cross-linking reaction within the one-component polymer.

The same temperature program was applied to the hybrid material **C4**, and the same general trend was observed (Figure 13). The ability to measure a storage modulus in the protected

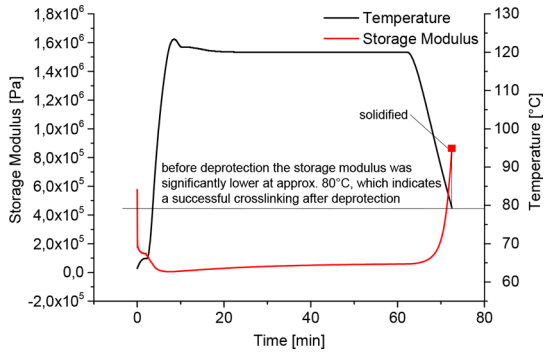

Figure 13. Temperature dependent rheology measurement of **C4**.

state of the sample below 80 °C compared to the solidification of the hybrid material, upon cooling within 10 min, indicates a successful and rapid DA cross-linking.

STEM images of microtome cutting slices (~20 nm depth) of **C3** were prepared to investigate the nanostructure of the hybrid material (Figure 14 and Figure S42). The images show a homogeneous distribution of **C6U** within the hydrogen bond motive functionalized polymer matrix. No agglomerates could be found, in neither a low nor a high magnification. Notice that the black lines in Figure 14 (left) belong to the TEM grid. An EDX spectrum of this sample was recorded to prove that the silica nanocages (**C6U**) are part of the microtome cutting slice (Figure S43).

Optical Microscope Images: Proof of Principle. Self-healing studies were performed applying a 1 cm × 1 cm × 1 mm sample by creating a cut of 5 mm through the entire specimen (Figure 15).

As mentioned above, **C1** and **C2** showed an inhomogeneous distribution of the urea group bearing spherosilicate **C6U**.

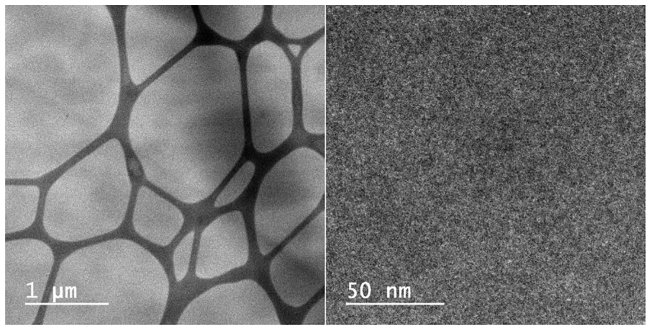

Figure 14. STEM images of microtome cutting slice (~20 nm depth) of **C3**.

Healing experiments were performed identically to the other samples: a cut was prepared, the interfaces were gently pressed together at room temperature, the samples were placed in an oven at 120 °C for 30 min, and treated at 70 °C for 20 h afterward. Figure S34 shows the control experiment with composite **C1**, which only consists of pBMA with the filler **C6U**. When the interfaces were pressed together at 30 °C, the hydrogen bonds of **C6U** provide close contact. By heating the sample to 120 °C, the material "healed" almost completely by simple flowing together of the polymer matrix. However, the material is significantly softer than the DA-containing hybrid materials. While **C1** "healed" because the material was heated above T_g, **C2** first seemed to heal quite efficiently, when heated to 120 °C because it seemed to behave like the pure polymer matrix (Figure S35). After heating to 70 °C for 20 h, the crack was still visible, which should be reasoned by a mismatch of the cut surfaces due to the lack of supramolecular forces.

C3 (Figure S36) healed equally to **C4**, which is discussed in the following section. As shown in Figure 15, composites **C4** and **C5** reveal a relatively high self-healing potential. After a macroscopic damage of several millimeters, the interfaces could be recombined at 30 °C. Because of a glue-like effect of hydrogen bonds, the specimens could recombine by gently pressing the two interfaces together at 30 °C (Figure 15, left d, right d)).

Healing the sample by thermal treatment led to the disappearance of the cut in sample **C4** (Figure 15, left f) and to reduction of the crack in sample **C5** (Figure 15, right, f). Therefore, the DA groups were de-cross-linked by heating the sample 30 min at 120 °C. Thus, linear polymer chains can move again, and a complete closure (**C4**) and partial closure (**C5**) of the cut occurs by the help of newly organized hydrogen bonds and re-formed DA product after cross-linking again at 70 °C within 20 h. The difference between **C4** and **C5** should be attributed to the urea groups within the polymer matrix, which lowers the mobility of the chains due to stronger interlock between filler and polymer compared to the amide.

4. CONCLUSIONS

Novel functional pBMA-based hybrid materials containing the DA moieties FMA and MiMA as well as hydrogen bond forming monomer **H1** or **H2** were synthesized. The linear polymers were prepared via living radical polymerizations ATRP or RAFT at 70 °C and characterized by ^{1}H NMR, IR, DSC, and SEC measurements. A homogeneous distribution of inorganic filler is ensured using spherosilicates modified with urea groups, which affords two H donors and one H acceptor. Self-healing was demonstrated using a FTIR, DSC, CP-MAS

DOI: 10.1021/acs.macromol.8b00601
Macromolecules XXXX, XXX, XXX−XXX

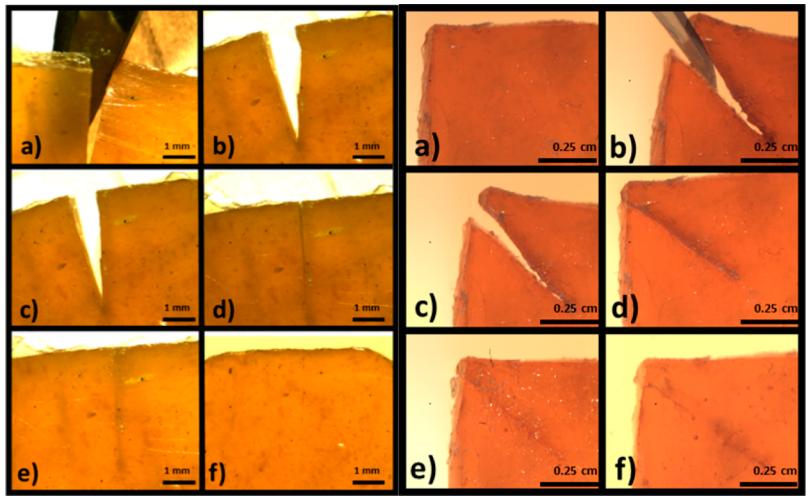

Figure 15. Microscope images of self-healing experiments on samples **C4** (left) and **C5** (right). **C4**: (a) cut through whole sample; (b, c) recombination of surfaces; (d) gently pressed together interfaces at 30 °C; (e) de-cross-linked at 120 °C and (f) cross-linked at 70 °C; **C5**: (a) initial sample; (b) cut through whole sample; (c) recombination of surfaces; (d) gently pressed together interfaces at 30 °C; (e) de-cross-linked at 120 °C and (f) cross-linked at 70 °C.

NMR, and an optical microscope. DSC measurements showed high endothermic peak areas between 120 and 200 °C for de-cross-linking of the DA bonds. Optical microscope images revealed a promising self-healing ability of the obtained materials. Cuts of 1 mm depth and at least 5 mm length could be healed completely. Localizing both Diels–Alder moieties within the matrix of the hybrid materials is superior compared to the Diels–Alder cross-linking between inorganic filler surface and organic matrix. Furthermore, placing hydrogen bonds within the polymers leads to a glue-like effect, which provides immediately close contact of the cut interfaces. This contact is a necessary condition for effective healing.

■ ASSOCIATED CONTENT

Supporting Information

The Supporting Information is available free of charge on the ACS Publications website at DOI: 10.1021/acs.macromol.8b00601.

^{1}H and ^{13}C NMR spectra of synthesized molecules (**1**–**10**) and polymers (**P1**–**P10**), DSC curves (second heating) of polymers **P6**–**P10**, IR spectra of composites **C1**–**C4**, DSC curves of **C1**–**C4**, microscope images of composites **C1**–**C3**, UV-vis spectra and time over conversion plot for **P8**, rheological measurement for **P8**, STEM images and EDX for **C3** (PDF)

■ AUTHOR INFORMATION

Corresponding Author

*E-mail: guido.kickelbick@uni-saarland.de (G.K.).

ORCID

Guido Kickelbick: 0000-0001-6813-9269

Notes

The authors declare no competing financial interest.

■ ACKNOWLEDGMENTS

We thank J. Schmauch for the STEM images of microtome cutting slices and the INM for providing access to the JEOL JEM-ARM 200F instrument.

■ REFERENCES

(1) Diesendruck, C. E.; Sottos, N. R.; Moore, J. S.; White, S. R. Biomimetic Self-Healing. *Angew. Chem., Int. Ed.* **2015**, *54*, 10428–10447.

(2) Tasdelen, M. A. Diels–Alder "click" reactions: recent applications in polymer and material science. *Polym. Chem.* **2011**, *2* (10), 2133–2145.

(3) Ruiz de Luzuriaga, A.; Martin, R.; Markaide, N.; Rekondo, A.; Cabanero, G.; Rodríguez, J.; Odriozola, I. Epoxy resin with exchangeable disulfide crosslinks to obtain reprocessable, repairable and recyclable fiber-reinforced thermoset composites. *Mater. Horiz.* **2016**, *3*, 241–247.

(4) Thakur, V. K.; Kessler, M. R. Self-healing polymer nanocomposite materials: A review. *Polymer* **2015**, *69*, 369–383.

(5) Zhong, N.; Post, W. Self-repair of structural and functional composites with intrinsically self-healing polymer matrices: A review. *Composites, Part A* **2015**, *69*, 226–239.

(6) Arslan, M.; Tasdelen, M. Polymer Nanocomposites via Click Chemistry Reactions. *Polymers* **2017**, *9*, 499.

(7) Adachi, K.; Achimuthu, A. K.; Chujo, Y. Synthesis of Organic-Inorganic Polymer Hybrids Controlled by Diels-Alder Reaction. *Macromolecules* **2004**, *37*, 9793–9797.

(8) Engel, T.; Kickelbick, G. Self-healing nanocomposites from silica – polymer core – shell nanoparticles. *Polym. Int.* **2014**, *63* (5), 915–923.

(9) Engel, T.; Kickelbick, G. Thermoreversible Reactions on Inorganic Nanoparticle Surfaces: Diels–Alder Reactions on Sterically Crowded Surfaces. *Chem. Mater.* **2013**, *25* (2), 149–157.

(10) Schäfer, S.; Kickelbick, G. Self-healing polymer nanocomposites based on Diels-Alder-reactions with silica nanoparticles: The role of the polymer matrix. *Polymer* **2015**, *69*, 357–368.

(11) Schäfer, S.; Kickelbick, G. Diels–Alder Reactions on Surface-Modified Magnetite/Maghemite Nanoparticles: Application in Self-Healing Nanocomposites. *ACS Appl. Nano Mater.* **2018**, *1*, 2640.

(12) Chuo, T.-W.; Liu, Y.-L. Preparation of self-healing organic–inorganic nanocomposites with the reactions between methacrylated polyhedral oligomeric silsesquioxanes and furfurylamine. *Compos. Sci. Technol.* **2015**, *118*, 236–243.

(13) Xu, Z.; Zhao, Y.; Wang, X.; Lin, T. A thermally healable polyhedral oligomeric silsesquioxane (POSS) nanocomposite based on Diels-Alder chemistry. *Chem. Commun.* **2013**, *49* (60), 6755–6757.

DOI: 10.1021/acs.macromol.8b00601
Macromolecules XXXX, XXX, XXX–XXX

(14) Engel, T.; Kickelbick, G. Furan-Modified Spherosilicates as Building Blocks for Self-Healing Materials. *Eur. J. Inorg. Chem.* **2015**, *2015* (7), 1226−1232.
(15) Nasresfahani, A.; Zelisko, P. M. Synthesis of a self-healing siloxane-based elastomer cross-linked via a furan-modified polyhedral oligomeric silsesquioxane: investigation of a thermally reversible silicon-based cross-link. *Polym. Chem.* **2017**, *8* (19), 2942−2952.
(16) Ciferri, A. Bond Scrambling and Network Elasticity. *Chem. - Eur. J.* **2009**, *15* (28), 6920−6925.
(17) Liu, C. K.; Yang, T. J.; Shen, J. S.; Lee, S. Some recent results on crack healing of poly(methyl methacrylate). *Eng. Fract. Mech.* **2008**, *75* (17), 4876−4885.
(18) Fang, X.; Zhang, H.; Chen, Y.; Lin, Y.; Xu, Y.; Weng, W. Biomimetic Modular Polymer with Tough and Stress Sensing Properties. *Macromolecules* **2013**, *46* (16), 6566−6574.
(19) Araya-Hermosilla, R.; Broekhuis, A. A.; Picchioni, F. Reversible polymer networks containing covalent and hydrogen bonding interactions. *Eur. Polym. J.* **2014**, *50*, 127−134.
(20) Araya-Hermosilla, R.; Lima, G. M. R.; Raffa, P.; Fortunato, G.; Pucci, A.; Flores, M. E.; Moreno-Villoslada, I.; Broekhuis, A. A.; Picchioni, F. Intrinsic self-healing thermoset through covalent and hydrogen bonding interactions. *Eur. Polym. J.* **2016**, *81*, 186−197.
(21) Willocq, B.; Khelifa, F.; Brancart, J.; Van Assche, G.; Dubois, Ph.; Raquez, J.-M. One-component Diels−Alder based polyurethanes: a unique way to self-heal. *RSC Adv.* **2017**, *7*, 48047−48053.
(22) Schäfer, S.; Kickelbick, G. Simple and high yield access to octafunctional azido, amine and urea group bearing cubic spherosilicates. *Dalton Trans* **2017**, *46* (1), 221−226.
(23) Pelagalli, R.; Chiarotto, I.; Feroci, M.; Vecchio, S. Isopropenyl acetate, a remarkable, cheap and acylating agent of amines under solvent- and catalyst-free conditions: a systematic investigation. *Green Chem.* **2012**, *14* (8), 2251.
(24) Kavitha, A. A.; Singha, N. K. Atom-Transfer Radical Copolymerization of Furfuryl Methacrylate (FMA) and Methyl Methacrylate (MMA): A Thermally-Amendable Copolymer. *Macromol. Chem. Phys.* **2007**, *208* (23), 2569−2577.
(25) Dispinar, T.; Sanyal, R.; Sanyal, A. A Diels-Alder/retro Diels-Alder strategy to synthesize polymers bearing maleimide side chains. *J. Polym. Sci., Part A: Polym. Chem.* **2007**, *45* (20), 4545−4551.
(26) Hasegawa, I.; Motojima, S. Dimethylvinylsilylation of $Si_8O_{20}^{8-}$ silicate anion in methanol solutions of tetramethylammonium silicate. *J. Organomet. Chem.* **1992**, *441* (3), 373−380.
(27) Dutkiewicz, M.; Maciejewski, H.; Marciniec, B.; Karasiewicz, J. New Fluorocarbofunctional Spherosilicates: Synthesis and Characterization. *Organometallics* **2011**, *30* (8), 2149−2153.
(28) Kötteritzsch, J.; Stumpf, S.; Hoeppener, S.; Vitz, J.; Hager, M. D.; Schubert, U. S. One-Component Intrinsic Self-Healing Coatings Based on Reversible Crosslinking by Diels-Alder Cycloadditions. *Macromol. Chem. Phys.* **2013**, *214* (14), 1636−1649.
(29) Chen, Y.; Kushner, A. M.; Williams, G. A.; Guan, Z. <34 Yulin Chen†, Aaron M. Kushner†, Gregory A. Williams and Zhibin Guan nchem.1314.pdf>. *Nat. Chem.* **2012**, *4*, 467−472.
(30) Beck, J. B.; Killops, K. L.; Kang, T.; Sivanandan, K.; Bayles, A.; Mackay, M. E.; Wooley, K. L.; Hawker, C. J. Facile Preparation of Nanoparticles by Intramolecular Crosslinking of Isocyanate Functionalized Copolymers. *Macromolecules* **2009**, *42* (15), 5629−5635.
(31) Flores, J. D.; Shin, J.; Hoyle, C. E.; McCormick, C. L. Direct RAFT polymerization of an unprotected isocyanate-containing monomer and subsequent structopendant functionalization using "click"-type reactions. *Polym. Chem.* **2010**, *1* (2), 213−220.
(32) Mido, Y. An infrared study of various dialkylureas in solution. *Spectrochim. Acta* **1973**, *29* (3), 431−438.
(33) Rao, C. N. R.; Chaturvedi, G. C.; Gosavi, R. K. Infrared spectra and configurations of alkylurea derivatives: Normal vibrations on N, N′-dimethyl- and tetramethylurea. *J. Mol. Spectrosc.* **1968**, *28* (4), 526−535.
(34) Mettler_Toledo, Interpreting DSC curves: Part 1: Dynamic measurementes. *User Com* **2000**, *11*, 1−26.

DOI: 10.1021/acs.macromol.8b00601
Macromolecules XXXX, XXX, XXX−XXX